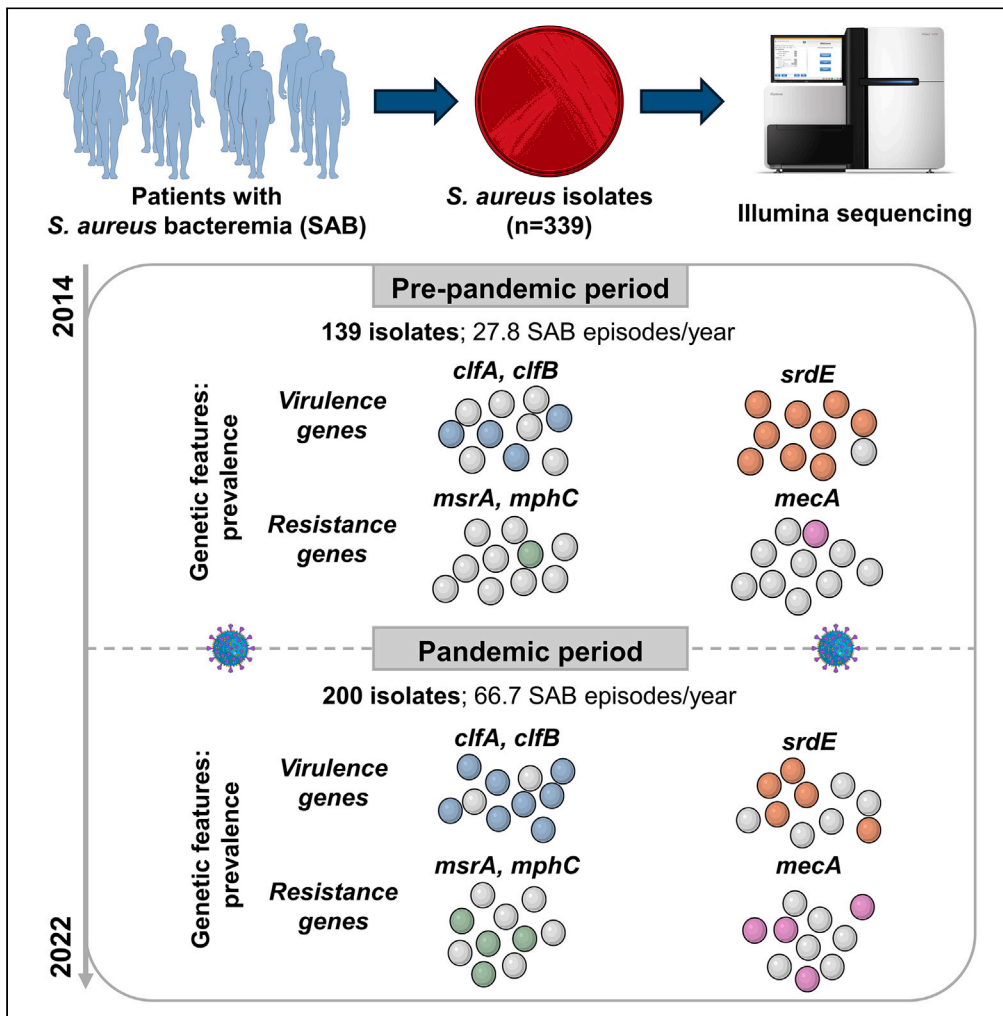


Article

Genomic analysis of *Staphylococcus aureus* isolates from bacteremia reveals genetic features associated with the COVID-19 pandemic



Miquel Sánchez-Osuna, Marc Pedrosa, Paula Bierge, ..., Ivan Erill, Oriol Gasch, Oscar Q. Pich

msanchezo@tauli.cat (M.S.-O.)
oquijada@tauli.cat (O.Q.P.)

Highlights

The incidence of *S. aureus* bacteremia increased during the COVID-19 pandemic

No emerging *S. aureus* lineages were detected during the pandemic era

Resistance to methicillin and macrolides rose in the pandemic years

Prevalence of fibrinogen-binding virulence factors increased during the pandemic



Article

Genomic analysis of *Staphylococcus aureus* isolates from bacteremia reveals genetic features associated with the COVID-19 pandemic

Miquel Sánchez-Osuna,^{1,2,*} Marc Pedrosa,³ Paula Bierge,^{1,2} Inmaculada Gómez-Sánchez,^{1,2} Marina Alguacil-Guillén,⁴ Mateu Espasa,⁴ Ivan Erill,^{5,6} Oriol Gasch,³ and Oscar Q. Pich^{1,2,7,*}

SUMMARY

Genomic analyses of bacterial isolates are effective to compare the prevalence of antibiotic resistance genes and virulence determinants in different contexts. This study provides a comprehensive genomic description of 339 *Staphylococcus aureus* strains isolated from patients with bacteremia (2014–2022). Nosocomial acquisition accounted for 56.6% of cases, with vascular catheters being the main infection source (31.8%). Fatality (27.4%), persistent bacteremia (19.5%), and septic emboli (24.2%) were documented. During the COVID-19 pandemic, *S. aureus* bacteremia episodes increased by 140%. Genetic features in pandemic isolates revealed higher prevalence of methicillin (*mecA*) and macrolide (*msrA* and *mphC*) resistance genes. Additionally, genes encoding clumping factors A and B, involved in fibrinogen binding, were more prevalent. This was linked to extensive macrolide use in COVID-19 accessory therapy and elevated fibrinogen levels in SARS-CoV-2 infection. These findings highlight *S. aureus* adaptation to COVID-19 selective pressures and the value of whole-genome sequencing in molecular epidemiology studies.

INTRODUCTION

Bacteremia is a life-threatening condition with high morbidity and mortality rates that can elicit a systemic host response known as sepsis.¹ These episodes often result in complicated bacteremia, usually defined by the presence of attributable mortality, the development of hematogenous embolisms (i.e., endocarditis, discitis, and osteomyelitis of systemic abscesses), or the persistence of viable bacteria in blood after three or more days after proper antibiotic treatment.² *Staphylococcus aureus* is among the top species causing bacteremia-associated mortality³ and persistent bacteremia,⁴ which in turn is linked to a higher risk of metastatic spread.⁵ There is increasing awareness that patients who survive sepsis often have long-term physical, psychological, and cognitive disabilities with significant health care and social implications.⁶

Several host factors such as certain comorbidities, the setting of the infection onset, and the severity of sepsis have been associated with the high mortality rates observed in *S. aureus* bacteremia.⁷ However, the patient's age is the most consistent predictor of mortality, with older patients being twice as likely to die.⁷ Also, certain strain characteristics such as methicillin resistance have also been shown to impact the clinical outcome.⁸ In contrast, the role of specific genetic traits of *S. aureus* in the evolution of bacteremia is much less understood. Recent studies suggest that *S. aureus* genetic factors predictive of infection evolution may be lineage specific, which would hinder their identification.⁹

S. aureus has also been described as a leading cause of secondary infection during past viral pandemics, significantly increasing patient mortality rates.¹⁰ In this regard, recent reports have noted a higher incidence of bacteremia by *S. aureus* at the beginning of the COVID-19 pandemic.¹¹ In the same line, our group has recently reported a rise of vascular catheter-related bacteremia in early 2020 and a significant increase in cases of *S. aureus* bacteremia.¹² However, while several studies have addressed the incidence, prevalence, and clinical outcomes of SARS-CoV-2 and *S. aureus* co-infection,¹³ the genomic differences between such strains and those isolated in the pre-pandemic years have not been explored.

¹Laboratori de Recerca en Microbiologia i Malalties Infeccioses, Hospital Universitari Parc Taulí, Institut d'Investigació i Innovació Parc Taulí (I3PT-CERCA), Universitat Autònoma de Barcelona, Sabadell, Spain

²Institut de Biotecnologia i Biomedicina, Universitat Autònoma de Barcelona, Cerdanyola del Vallès, Spain

³Servei de Malalties Infeccioses, Hospital Universitari Parc Taulí, Institut d'Investigació i Innovació Parc Taulí (I3PT-CERCA), Universitat Autònoma de Barcelona, Sabadell, Spain

⁴Servei de Microbiologia, Hospital Universitari Parc Taulí, Institut d'Investigació i Innovació Parc Taulí (I3PT-CERCA), Universitat Autònoma de Barcelona, Sabadell, Spain

⁵Department of Biological Sciences, University of Maryland Baltimore County, Baltimore, MD, USA

⁶Departament d'Enginyeria de la Informació i de les Comunicacions, Universitat Autònoma de Barcelona, Cerdanyola del Vallès, Spain

⁷Lead contact

*Correspondence: msanchezo@tauli.cat (M.S.-O.), oquijada@tauli.cat (O.Q.P.)

<https://doi.org/10.1016/j.isci.2024.110402>



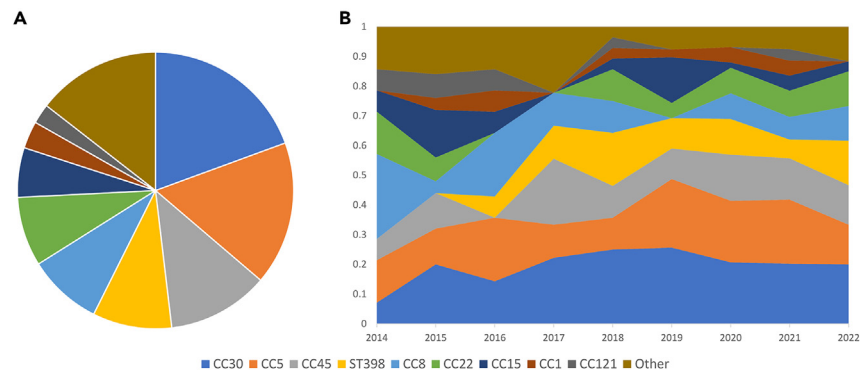


Figure 1. Overview of *S. aureus* lineages in our collection

(A) Pie chart depicting global *S. aureus* lineage frequencies in our collection.

(B) Graphical representation of *S. aureus* lineage frequencies over years. Lineages with less than 5 representatives are collected under the umbrella term “Other”.

Here, we investigated the clinical aspects, epidemiology, and genomic features of 339 *S. aureus* strains isolated from patients with bacteremia at the Parc Tauli University Hospital before and during the COVID-19 pandemic (2014–2022). This analysis allowed us to shed light into significant associations between *S. aureus* lineages, antibiotic resistance genes, virulence factors, and the clinical outcome of bacteremia. Comparative genomics analysis pointed out that some virulence factors and antibiotic resistance genes were enriched in pandemic *S. aureus* isolates.

RESULTS

Cohort description

We identified 339 consecutive adult patients diagnosed with *S. aureus* bloodstream infection between 2014 and 2022 (Data S1). Most of them were male (69.3%) and the mean age was 63.7 ± 19.9 years. The calculated modified Charlson score was greater or equal than 4 in 64.0%. The most frequent clinical conditions detected were diabetes (31.6%), the presence of a foreign device (25.4%), ischemic heart disease (17.7%), congestive heart failure (16.5%), solid neoplasm (15.3%), peripheral arteriopathy (12.7%), and chronic obstructive pulmonary disease (10.0%). Acquisition was nosocomial in 56.6%, while 27.4% were community acquired and 16.0% healthcare related. Regarding the primary source of infection, vascular catheters (31.8%) and skin infections (18.0%) were predominant, followed by pneumonia (9.4%). As far as 30.7% episodes were of unknown origin ($n = 104$). Antibiotic susceptibility tests indicated resistance to penicillin (86.1%), erythromycin (30.4%), clindamycin (20.9%), ciprofloxacin (16.8%), levofloxacin (15.3%), oxacillin (13.9%), amoxicillin/clavulanic acid (13.6%), gentamicin (10.0%), tetracycline (2.9%), cotrimoxazole (1.5%), linezolid (0.3%), and rifampicin (0.3%) in our strains (Data S1). Resistance to daptomycin, vancomycin, and teicoplanin was not observed.

Regarding clinical outcomes, 93 cases were fatal (27.4%) and the median time to patient’s death was 20 (interquartile 25 [IQ25] = 8, interquartile 75 [IQ75] = 37) days (Data S1). Fatal bacteremia episodes showed to be significantly associated with age, modified Charlson, sepsis, congestive heart failure, immunosuppressive chemotherapy treatment, endocarditis, and the presence of a cardiac device (Table S1). Of note, catheter-related bacteremia episodes were less lethal ($p < 0.05$) (Table S1). On the other hand, persistent bacteremia was observed in 19.5% of episodes, with the median duration being 43 (IQ25 = 24, IQ75 = 67.5) days (Data S1). Persistent infections were significantly associated with sepsis (Table S1). Pneumonia-originated bacteremia never resulted in persistent infections or septic emboli infections ($p < 0.05$) (Table S1). Septic emboli were diagnosed in 24.2% (Data S1), which were more prevalent in community-acquired infections ($p < 0.05$) (Table S1). Septic emboli infections were significantly associated with infective endocarditis episodes (Table S1).

Isolate typing

The multilocus sequence typing software classified our *S. aureus* isolates in 24 different lineages (Figure 1A and Data S1). The major identified lineages were CC30 (19.5%), CC5 (17.1%), CC45 (12.1%), ST398 (8.8%), CC8 (8.8%), CC22 (8.0%), and CC15 (5.9%). 18 isolates could not be classified into a known sequence type. The distribution of lineages remained relatively stable over the years of study (Figure 1B).

We found significant associations between specific lineages and clinical data. CC5 and CC8 strains were more frequently recovered from patients with pneumonia-related bacteremia, while CC30 isolates were more prevalent among bacteremia from surgical site infections ($p < 0.05$) (Data S2 and Table S2). Although we did not find any significant association, CC1 and CC8 infections showed the highest mortality rates (45.4% and 40.0%, respectively). CC15, CC30, CC45, CC21, and ST398 lineages generated persistent infection with frequencies ranging from 20.0% to 25.0%, while CC1 (9.1%) and CC22 (7.4%) were the lineages generating fewer persistent infections. The strains most frequently associated with septic emboli were CC15 and CC45 (30.0% and 34.1%), while those that formed the least were CC1 and CC8 (9.1% and 10.0%) (Data S1).

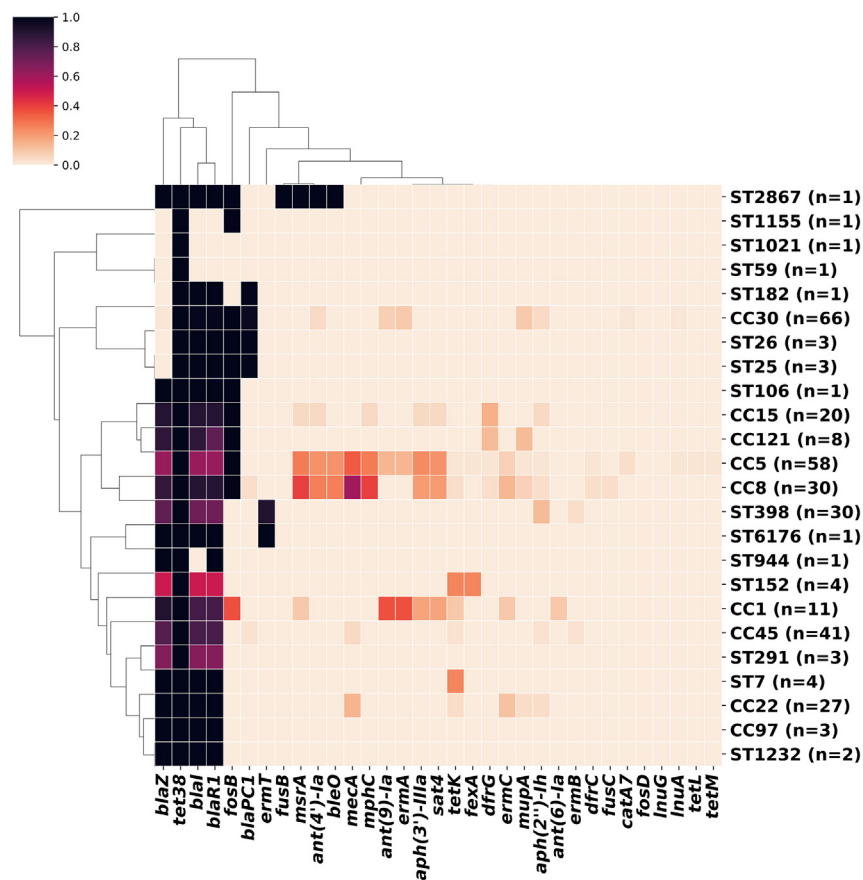


Figure 2. Clustered heatmap representing the frequency of abricate-predicted ARGs for all *S. aureus* lineages

Cells are colored from pale orange (0%) to black (100%). Samples were clustered and visualized using the Seaborn clustermap function. Isolates with unknown lineage were not included.

Methicillin-resistant *Staphylococcus aureus* (MRSA) strains belonged more frequently to CC5 (42.5%) and CC8 (38.3%) lineages ($p < 0.05$) (Data S2 and Table S2), but methicillin resistance was also found in CC22 (8.5%) and CC45 (4.2%) strains, as well as unknown lineages (6.5%) (Data S1). The vast majority (95.7%) of SCCmec cassettes were grouped into type IV, except for two SCCmec cassettes classified as type V (Data S1). SCCmec type IVc was associated with CC5 and CC8, while SCCmec type IV was linked to CC5 and CC22 clones ($p < 0.05$) (Data S2 and Table S2). In our collection, we did not find any association of MRSA strains with mortality (Matthews correlation coefficient [MCC] = 0.06).

Our analysis predicted that 13 isolates from our collection were *agr* negative. Among the *agr*-positive strains, 48.5% were classified as type I, 26.1% type II, 22.1% type III, and 3.3% type IV (Data S1). We observed a biased distribution of lineages regarding the *agr* types II and III ($p < 0.05$) (Data S2). Specifically, we found that type II *agr* was associated with CC5 and CC15 isolates, while type III was almost exclusive of CC30 clones ($p < 0.05$) (Table S2). Finally, our typing analysis revealed 123 different *spa* types (Data S1), with t012 significantly associated with CC30 isolates, t002 and t067 with CC5, t008 with CC8, t084 with CC15, and t1451 with ST398 (Data S2 and Table S2).

Antibiotic resistance genes

We identified homologs to 34 different antibiotic resistance gene (ARG) families conferring resistance to clinically relevant antibiotics (Figure 2 and Data S1). Homologs of the *mecA* gene were found in 47 strains (13.9%) and they were associated primarily with CC5 and CC8 strains ($p < 0.05$) (Data S2 and Table S2).

Homologs of genes related to tetracycline, β -lactams, and fosfomycin resistance were the most prevalent. Homologs of *tet38* were identified in all isolates, of complete *blaI-blaR-blaZ* clusters in 279 strains (82.3%) and of *fosB* in 206 strains (60.2%). We found that the *bla*_{PC1} variant was mainly associated with strains belonging to the CC30 lineage ($p < 0.05$) (Data S2 and Table S2). All isolates belonging to CC5, CC8, CC15, CC30, and CC121 lineages encoded a *fosB* gene homolog. In contrast, CC22, CC45, and ST398 clones did not present any fosfomycin resistance gene homologs (Table S2).

In addition, we identified homologs to three different groups of genes conferring macrolide resistance: several *erm* variants encoding 23S rRNA methylases (19.5%), the ABC-F type ribosomal protection encoding gene *msrA* (10.0%), and the phosphotransferase gene *mphC* (9.4%).

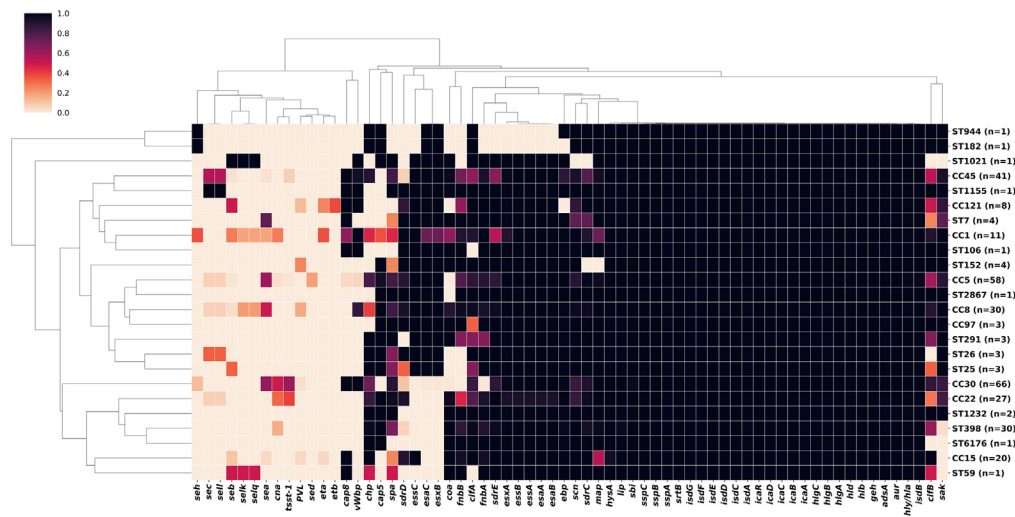


Figure 3. Clustered heatmap representing the frequency of abricate-predicted VFs for all *S. aureus* lineages

Cells are colored from pale orange (0%) to black (100%). Samples were clustered and visualized using the Seaborn clustermap function. Isolates with unknown lineage were not included.

We observed a strong correlation between homologs of *mphC* and *msrA* (MCC = 0.97), which were significantly associated with CC5 and CC8 lineages (Data S2 and Table S2). In addition, almost all strains carrying *ermT* belonged to the ST398 sequence type ($p < 0.05$) (Data S2 and Table S2). Homologs of *ermA* were associated with CC1 and CC5 while *ermC* homologs were linked to CC8 clones ($p < 0.05$) (Data S2 and Table S2). We also detected a biased distribution of the aminoglycoside nucleotidyltransferase genes *ant(4')-Ia* (9.1%) and *ant(9)-Ia* (5.9%) as well as of the aminoglycoside phosphotransferase genes *aph(3')-IIIa* (7.4%) and *aph(2'')-Ih* (4.4%) (Data S2). Specifically, *ant(4')-Ia* gene homologs were significantly associated with CC5 and CC8 strains, *ant(9)-Ia* with CC1 and CC5, *aph(3')-IIIa* with CC5 and CC8, and *aph(2'')-Ih* with ST398 (Table S2). Homologs of the bleomycin resistance gene *bleO* (7.4%) showed a positive correlation with *ant(4')-Ia* (MCC = 0.89) and were also linked to CC5 and CC8 clones ($p < 0.05$) (Data S2, and Table S2). Finally, homologs of the *mupA* gene (3.8%), conferring mupirocin resistance, were significantly associated with CC30 isolates (Data S2 and Table S2).

ResFinder identified mutations associated with ciprofloxacin resistance in 164 strains (48.4%) (Data S1). Prevalent mutations included S84L *gyrA* ($n = 48$), I45M *griA* ($n = 42$), and S80F *griA* ($n = 38$). The D432N mutation in the *griB* gene was also predicted to confer ciprofloxacin resistance, albeit to a lesser extent ($n = 10$). Of note, some isolates harbored multiple instances of these mutations simultaneously. Per lineages, the I45M *griA* variant was significantly associated with CC45 clones, S80F *griA* with CC5, S80Y *griA* with CC8, and S84L *gyrA* with both CC5 and CC8 isolates (Table S2). In addition, a V588F *ileS* mutation conferring mupirocin resistance and a S464P *rpoB* mutation conferring rifampicin resistance were predicted in two single isolates (Data S1).

Finally, we computed MCC to compare empirical antibiotic susceptibility testing results with *in silico* predicted resistance. We observed strong correlation values for predicting amoxicillin/clavulanic acid (MCC = 0.91), penicillin (MCC = 0.84), rifampicin (MCC = 1), oxacillin (MCC = 0.92), and erythromycin (MCC = 0.89) resistance. Notably, the presence of the *mecA* gene was highly correlated with amoxicillin/clavulanic acid resistance (MCC = 0.91). However, lower MCC values were observed for ciprofloxacin/levofloxacin (MCC = 0.57), gentamicin (MCC = 0.60), and cotrimoxazole (MCC = 0.28) resistance. Predicted resistance for clindamycin (MCC = 0.03) and tetracycline (MCC = 0) were independent of antibiotic susceptibility testing results. Tetracycline resistance prediction showed very different MCC values when evaluating *tetK* (MCC = 0.73), *tetL* (MCC = 0.31), *tetM* (MCC = 0.31), and *tet38* (MCC = 0) genes. Also, while 9 linezolid-resistant strains were isolated, linezolid resistance genes were not predicted.

Virulence factors

The presence of virulence factors contributing to *S. aureus* pathogenicity and invasiveness was predicted (Figure 3 and Data S1). All isolates from our collection carried homologs of the *cap* gene cluster responsible for the synthesis of capsular polysaccharide. Capsular polysaccharide serotype 8 was significantly more prevalent in CC15, CC30, CC45, and CC121 lineages (Data S2 and Table S2), while serotype 5 was mainly found at CC5, CC8, CC22, and ST398 clones. Homologs of the immune evasion cluster (IEC) (*sak*, *chp*, and *scn*) and *sbi*, also involved in immune system evasion, were present in 73.1%–99.4% of the isolates. The *sak* gene was not found in ST398 isolates. Similarly, 99.7% of the isolates carried the *isdA-G* gene homologs, which confer resistance to killing by human lactoferrin. The intracellular adhesion locus, involved in cell-cell adherence and biofilm formation, was detected in all strains. Homologs of genes coding for several microbial surface components recognizing adhesive matrix molecules (MSCRAMMs) were also detected, although to different extents: *ebp* (95.3%), *eap/map* (93.5%), *sdrC* (92.0%), *sdrE* (87.6%), *clfA* (86.1%), *fmbA* (74.6%), *clfB* (68.4%), *fmbB* (62.2%), *sdrD* (53.7%), von Willebrand factor-binding protein (*vWbp*)

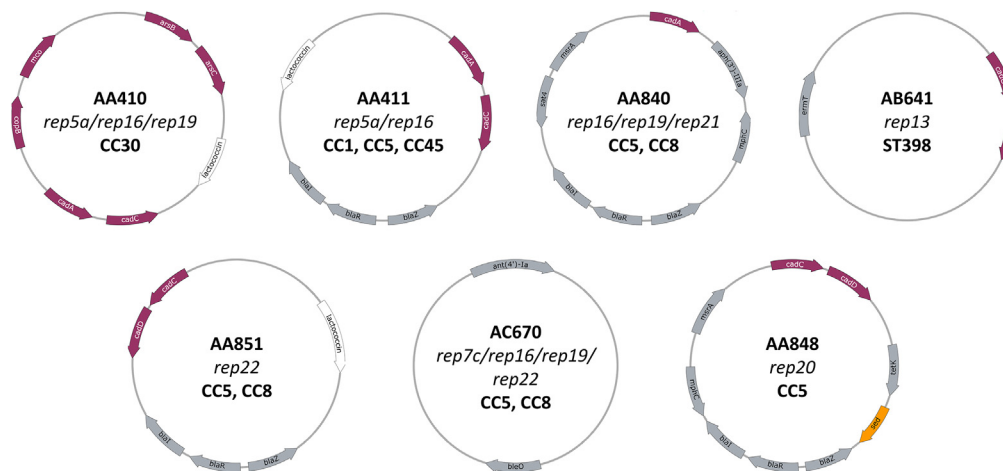


Figure 4. Schematic representation of the most abundant plasmids in our collection

Gene coloring depicts ARGs (gray), VF (orange), heavy metal resistance genes (purple), and lactococcin synthesis genes (white). Rep types and lineage associations are also included. Only plasmids harbored in more than 15 isolates were included.

(47.8%), and *cna* (15.9%). Specifically, we found that the secreted *vWbp* was more prevalent in CC1, CC8, CC30, CC45, and CC121 lineages while the *cna* gene was associated with CC30 clones ($p < 0.05$) (Data S2 and Table S2).

Almost all isolates carried homologs of the genes encoding the α -, β - and δ -hemolysins (*hla*, *hlb*, *hlgABC*, and *hld*). Genes responsible for the formation of type VII secretion systems (T7SSs), *esa*, *ess*, and *esx*, were also widespread in our collection. Enterotoxin-encoding genes (*sea*, *seb*, *sec*, *sed*, *seh*, *selk*, *sell*, and *selq*) showed markedly different frequencies ranging from 31.0% (*sea*) to 2.9% (*selk* and *selq*) and significantly biased distributions among different lineages (Data S2). Specifically, CC1 strains were associated with *seb*, *seh*, *selk*, and *selq*; CC5 with *sea* and *sed*; CC8 with *sea*, *selk*, and *selq*; CC30 with *sea* and *seh*; CC45 with *sea*, *sec*, and *sell*; and CC121 with *seb* ($p < 0.05$) (Table S2). Of note, *sec* and *sell* genes were totally correlated (MCC = 1.0). We also detected the presence of the toxic shock syndrome toxin-1 (*tsst-1*) gene homologs in 56 isolates (16.5%), which were linked to CC22 and CC30 ($p < 0.05$) (Data S2, and Table S2). In addition, 11 isolates were predicted to encode the Pantone-Valentine leukocidin (PVL) genes (*lukF* and *lukS*) with a linkage to CC8 strains (Data S2, and Table S2). Finally, we also found homologs of the toxin-encoding genes *eta* (2.1%) and *etb* (0.9%) in our strains.

Plasmids

We identified 51 different plasmids distributed in 256 isolates (75.5%) (Figure 4, and Data S1). Among them, the vast majority (52.8%) presented a single plasmid, but we also found strains with two (18.3%), three (3.2%), or four (1.2%) plasmids.

The core proteome of the most prevalent plasmid, AA410 ($n = 72$; *rep5a/rep16/rep19*), showed heavy metal resistance (*arsB*, *arsC*, *cadA*, *cadC*, *copB*, and *mco*) and lactococcin synthesis genes (Table S3). This plasmid was linked to CC30 strains ($p < 0.05$) (Data S2, and Table S2). Plasmid AA411 ($n = 56$; *rep5a/rep16*) harbored the *blaI-blaR-blaZ* cluster for penicillin resistance, a cadmium resistance cluster (*cadC*, *cadD*), and lactococcin synthesis genes (Table S3). In this case, AA411 plasmids were significantly associated with CC1, CC15, and CC45 (Data S2 and Table S2). Plasmid AA840 ($n = 33$; *rep16/rep19/rep21*), encoding *cadA* gene for cadmium resistance and several ARGs (*blaI-blaR-blaZ*, *aph(3')-IIIa*, *mphC*, *msrA*, and *sat4*) (Table S3), was more prevalent among CC5 and CC8 isolates ($p < 0.05$) (Data S2 and Table S2) and showed a positive correlation with MRSA strains (MCC = 0.73). Also, significantly associated with these lineages (Data S2 and Table S2) was the AA851 plasmid ($n = 22$, *rep22*), which harbored cadmium resistance genes (*cadC*, *cadD*), the *blaI-blaR-blaZ* cluster, and genes for lactococcin synthesis (Table S3). On the other hand, the plasmid AB641 ($n = 25$; *rep13*), which was almost exclusively detected in isolates from the ST398 lineage ($p < 0.05$) (Data S2, and Table S2), carried two cadmium resistance genes (*cadC*, *cadD*) and the macrolide resistance gene *ermT* (Table S3). Finally, plasmid AC670 ($n = 19$; *rep7c/rep16/rep19/rep22*) encoded genes conferring antimicrobial resistance (*ant(4')-Ia*, *bleO*); and plasmid AA848 ($n = 15$; *rep20*) carried several ARGs (*blaI-blaR-blaZ*, *mphC*, *msrA*, and *tetK*), two cadmium resistance loci (*cadC*, *cadD*), and the staphylococcal enterotoxin D-encoding (*sed*) gene (Table S3). AC670 plasmids were associated with CC5 and CC8 clones while AA848 plasmids were linked to CC5 clones ($p < 0.05$) (Data S2, and Table S2).

We also predicted other less-abundant plasmids, carrying other genes conferring resistance to aminoglycosides (*ant(6)-Ia*, *aph(2'')-Ih*), macrolides (*ermA*, *ermB*, *ermC*, *msrA*, and *mphA*), tetracycline (*tetK*), chloramphenicol (*catA7*), lincosamides (*lnuA*), and trimethoprim (*dfrG*). The exfoliative toxin B-encoding gene (*etb*) was also annotated in three plasmids (Table S3).

Overall, our results showed that *ant(6)-Ia*, *aph(3')-IIIa*, *catA7*, *ermC*, *lnuA*, *mphC*, *msrA*, and *sat4* genes were exclusively plasmid borne in our collection (Figure S1). Likewise, *mupA* (92.3%), *ant(4')-Ia* (90.3%), *bleO* (88.0%), *ermT* (80.6%), and *tetK* (77.8%) genes were also much more

prevalent in plasmids than in chromosomes. Similarly, around 50% of the *blaI-blaR-blaZ* cluster was detected in plasmids. In contrast, several abundant genes such as *ant(9)-la*, *ermA*, *fosB*, *mecA*, or *tet38* were always chromosomally encoded (Figure S1). Finally, the virulence genes *sed* and *etb* were found to be exclusively plasmid borne.

Prophages

We predicted 369 different prophage clusters in 336 isolates (97.6%) (Data S1). The majority presented one (28.6%) or two (28.9%) prophages, but we also found strains with three (21.5%), four (12.1%), five (7.4%), six (0.9%), or even seven (0.6%) prophage sequences.

Prophage clusters from the integrase group 3 (Sa3) were predominant in our collection ($n = 43$). Some of them ($n = 15$) carried homologs of complete IEC (*scn*, *chp*, and *sak*). Enterotoxin A-encoding gene (*sea*) was predicted in six of them and *tsst-1* was found in one cluster (Table S4). Of note, different Sa3-prophage clusters (1, 15, 29, and 55) showed a biased distribution in our collection (Data S2). Specifically, cluster 1 was associated with CC30, cluster 15 with ST398, cluster 29 with CC5, and, finally, cluster 55 with CC30 and ST398 strains ($p < 0.05$) (Table S2).

We further identified some prophage clusters ($n = 26$) of the integrase group 2 (Sa2), two of them encoding *sea* and *tsst-1* genes. We also predicted 24 prophage clusters from integrase group 1 (Sa1); 22 from integrase group 5 (Sa5), with two harboring *sec* and *sell* genes; and 17 from integrase group 6 (Sa6). Prophages from integrase group 7 (Sa7) and 9 (Sa9) were also identified but to a lesser extent. Finally, 221 prophage clusters did not present any integrase gene. Among those, 14 clusters carried a complete IEC and 10 harbored the *sea* gene (Table S4).

No ARGs were detected in the predicted prophage genomes

Pandemic-associated features

We identified 139 and 200 consecutive adult patients diagnosed with bloodstream infection by *S. aureus* before and after March 14th 2020, respectively (Data S1). Of note, 31.5% of the patients identified in the pandemic period also tested positive for SARS-CoV-2 (Data S1). In the pre-pandemic years, we detected 27.8 episodes of *S. aureus* bacteremia per year in our hospital rising to 66.7 during the pandemic. In such years, we observed an increase of nosocomial infections, from 69 episodes in the pre-pandemic years to 119 during the COVID-19 pandemic. Accordingly, there was a significant reduction in community-acquired *S. aureus* bacteremia (Table S5). Specifically, cases of *S. aureus* peripheral catheter-related bacteremia were significantly more prevalent and we also found 2.5 times more episodes of bacteremia originating from surgical sites (Table S5). We also identified a significant increase of MRSA infections ($p < 0.05$) and diagnosed 2.8 times more endocarditis cases (Table S5).

Statistical analysis on pre- and pandemic strains revealed significant genetic differences between these two *S. aureus* populations. We observed a strong increase of strains carrying genes encoding the clumping factors A (*clfA*, $p = 2.1e^{-03}$) and B (*clfB*, $p = 2.3e^{-05}$) (Table S5). Clumping factors A and B are MSCRAMMs that bind fibrinogen, which is found at high levels upon SARS-CoV-2 infection.¹⁴ In contrast, we found a significant reduction of strains encoding the *sdrE* gene, which is also classified as MSCRAMM (Table S5). However, the presence of *clfA*, *clfB*, and *sdrE* genes in *S. aureus* co-infecting COVID-19 patients had no impact on the clinical outcome of bacteremia (Table S6). On the other hand, we noticed a rise in several antibiotic resistance genes during those years. Specifically, the macrolide resistance *msrA* and *mphC* genes as well as the methicillin resistance *mecA* gene showed a significant increase during the pandemic years (Table S5). This led to a significant increase in resistance to erythromycin, oxacillin, and amoxicillin/clavulanic acid (Table S5). Of note, macrolides were extensively used as accessory therapy for COVID-19 in patients.¹⁵

These trends were not attributable to a shift in lineage distribution, as the frequency of lineages throughout the pandemic period could not be distinguished from those of the pre-pandemic era ($p > 0.05$). Similarly, core genome phylogenetic analysis did not reveal the presence of emerging sub-lineages within the major lineages during the pandemic years (Figure S2). Instead, our findings are indicative of convergent selection for the presence of these genes across multiple lineages, suggesting a widespread phenomenon rather than the emergence of particular lineages (Table S7).

DISCUSSION

Global insights into *S. aureus* clinics, antibiotic resistance, and virulence

Genomics enables unraveling the genetic makeup of pathogens, providing insights into virulence factors, antibiotic resistance mechanisms, and the overall pathogenic potential of bacteria. This information is crucial for the development of targeted diagnostics, treatment strategies, and preventive measures. The use of genomics also allows tracking the spread of specific strains and identifying emerging threats, contributing to the surveillance and control of infections. Here, using a collection of 339 *S. aureus* isolates from patients with bacteremia, we unveiled important insights into the clinical and genomic features of these bacterial pathogens (Table 1).

Our cohort confirms the trends regarding the clinical picture of *S. aureus* bacteremia observed in previous reports.¹⁶ Although significant changes in the characteristics and management of *S. aureus* bacteremia have been described, associated mortality remains stable and close to 20%–30% in most previous reports.¹⁷ One possible explanation is that the progressive increase of healthcare-acquired and venous catheter-associated episodes, which are features usually related to lower risk for death, compensates for progressive population aging and increase of associated comorbidities.⁷

In our hospital, we identified *S. aureus* lineages mirroring those previously reported in Spain¹⁸ and in other countries^{19,20} (Figure 1), suggesting a shared genetic heritage and potentially common evolutionary pathways. Pérez-Montarelo and colleagues analyzed strains isolated

Table 1. Summary of the significant associations between the most abundant *S. aureus* lineages with all the clinical and genetic data

Lineage	Clinical features	Gene types	Antibiotic resistance genes	Virulence factors	Plasmids	Prophages
CC1			<i>ant(9)-Ia, ermA</i>	<i>seb, seh, selk, selq</i>	AA411	
CC5	Pneumonia- originated bacteremia	SCCmec IVc, <i>agr</i> type II, <i>spa</i> t002, <i>spa</i> t067	<i>ant(4)-Ia, ant(9)-Ia, aph(3)-IIIa, bleO, ermA, fosB, mecA, mphC, msrA, S84L gyrA, S80F grlA</i>	<i>cap5, sea, sed</i>	AA840, AA851, AC670, AA848	Cluster_29 (Sa3)
CC8	Pneumonia- originated bacteremia	SCCmec IVc, <i>spa</i> t008	<i>ant(4)-Ia, aph(3)-IIIa, bleO, ermC, fosB, mecA, mphC, msrA, S84L gyrA, S80Y grlA</i>	<i>cap5, sea, selk, selq, PVL</i>	AA840, AA851, AC670	
CC15		<i>agr</i> type II, <i>spa</i> t084	<i>fosB</i>	<i>cap8</i>	AA411	
CC22		SCCmec IV		<i>cap5, tsst-1</i>		
CC30	Bacteremia from surgical site infections	<i>agr</i> type III, <i>spa</i> t012	<i>blaZPC1, fosB, mupA</i>	<i>cap8, sea, seh, tsst-1</i>	AA410	Cluster_1 (Sa3), cluster_55 (Sa3)
CC45			145M <i>grlA</i>	<i>cap8, sea, sec, sell</i>	AA411	
CC121			<i>fosB</i>	<i>cap8, seb</i>		
ST398		<i>spa</i> t1451	<i>aph(2)-Ih, ermT</i>	<i>cap5</i>	AB641	Cluster_15 (Sa3), cluster_55 (Sa3)

across various Spanish hospitals spanning 2002 to 2017.¹⁸ Our study, conducted between 2014 and 2022, complements this report and broadens its scope into the pandemic period, offering compelling observations on the evolutionary trends of *S. aureus* clones. Specifically, we observed an increase of ST398 lineages, heightening from 2.4%¹⁸ to a mean prevalence of 8.8% in our isolates. Importantly, the prevalence of this lineage in our collection ranged from 0% (2014 and 2015) to 15% (2022). These results highlight the spread of ST398 lineage in hospital settings, confirming the need to focus on the mechanisms involved in the epidemiological success of ST398 in humans, as previously suggested²¹ (Figure 1). Previous work associated the gradual spread of ST398 isolates in humans with the acquisition of mobile genetic elements, particularly Sa3-prophages carrying IEC genes.²² Our results agree with these reports, as we have identified a sequence of an Sa3-prophage associated with ST389 clones, encoding the IEC genes and the SEA toxin (Table S4).

Despite possible associations between genotypes and certain complications, the role of *S. aureus* genetic factors in the evolution of bacteremia is still poorly understood. Indeed, the combination of multiple factors, including the host immune response, patient's comorbidities, or the treatment strategies, is at play in determining the clinical outcome of bacteremia. CC1, CC5, CC8, CC22, and CC30 lineages have been associated with increased risk of complications.²³ In contrast, more recent studies did not find any apparent association between clonality and poorer outcomes.²⁴ Our study is in line with the latter since we did not find significant associations between the different isolates from our collection and clinical outcome. However, there is a trend for the CC1 and CC8 strains to cause fatal infections. On the other hand, we identified associations between the different lineages and the focus of infection. Specifically, CC5 and CC8 clones were correlated with pneumonia-originated bacteremia, as deduced from previous reports,²⁵ and CC30 with surgical site infections (Tables 1 and S2). Of note, bloodstream infections originating from CC5 and CC8 lineages were diagnosed later (median duration of 14 days and 21 days upon admission, respectively) as compared to CC30 (median duration of 10.7 days upon admission). This different epidemiology likely reflects the different infection sources associated with these lineages. Thus, surgical site infections are often linked to clones prevalent in community settings, while bacteremia episodes from nosocomial pneumonia are associated with MRSA strains.

MRSA poses a significant public health concern due to its ability to cause infections that are challenging to treat, showing higher mortality than methicillin-susceptible *Staphylococcus aureus* (MSSA) infections.²⁶ In Spain, the prevalence of methicillin resistance among *S. aureus* isolates is around 20%–25%,^{18,27} while the incidence of MRSA infections in our hospital showed to be 13.9% (Figure 2). Of note, we did not find associations with mortality and MRSA strains. In accordance with some reports, most of our MRSA isolates belonged to CC5 or CC8 strains.²⁸ These lineages were also the ones accumulating more antibiotic resistance genes (Figure 2, and Table 1), as previously stated.²⁹ Genes predicted to confer resistance to tetracycline and β -lactams were the most prevalent in our isolates (Figure 2). However, the results for tetracycline did not align well with the patterns observed *in vitro* by broth microdilution tests. The *tet38* gene, which was present in almost all strains, is known to confer tetracycline resistance when overexpressed,³⁰ but its mere presence does not necessarily indicate resistance to this class of antibiotics.

S. aureus is known for its pathogenic potential, primarily attributed to a diverse set of virulence factors. As previously elucidated, the *agr* groups and capsular polysaccharide serotypes were associated with *S. aureus* clonality (Figure 3 and Table 1).³¹ Several genes involved in immune system evasion (*adsA, aur, sbi, ssl, sspA, and sspB*), lactoferrin resistance (*isdA-G*), adhesion (*ica*), T7SS formation (*esa, ess, and esx*), some MSCRAMMs (*ebp, eap/map, and sdrC*), and hemolysins were found in virtually all strains (Figure 3), similar to previous reports.³² IEC is an immune response cluster harboring *chp, scn, and sak* genes which is typically encoded by β -hemolysin converting bacteriophages.³³ This is partially paralleled in our isolates, in which we predicted 61.7% of complete IEC clusters in prophage regions (Table S4). In contrast to many other bacterial pathogens, *S. aureus* produces a wide array of toxins.³⁴ In our hospital, besides hemolysins, the most abundant

predicted toxins were the exotoxins SEA (31.0%) and TSST-1 (16.5%), the latter being the major cause of toxic shock syndrome (Figure 3). SEA is the most common staphylococcal enterotoxin³⁵ and is also reported to be encoded by a prophage.³⁶ In our isolates, only 53.8% of sea genes were predicted in prophage regions (Table S4), hereby indicating that we could be underestimating prophage regions. Finally, we found 11 PVL-positive strains (3.2%) (Figure 3). PVL is a pore-forming leukotoxin produced by 2%–3% of *S. aureus* isolates,³⁷ which has been traditionally used as an indicator of community-acquired MRSA strains.³⁸ However, some recent studies found that PVL may not be a reliable marker because it is being reported in nosocomial MRSA infections.³⁹ Paralleling these reports, we found 4 non-community MRSA harboring PVL suggesting a possible spread of these strains in hospitals.

Changes in molecular characteristics of pandemic *S. aureus* isolates

Understanding the interplay between viral and bacterial infections, including the prevalence and impact of *S. aureus* in COVID-19 cases, is important for effective patient care and public health measures. Several studies underscored a higher incidence of bacteremia by *S. aureus* at the COVID-19 pandemic.¹¹ In keeping with this, the episodes of *S. aureus* bacteremia per year doubled in our hospital during the pandemic. Concomitantly, we found a rise in nosocomial infections, particularly those originating from catheters and surgical sites. The increase of catheter-related bacteremia during the COVID-19 epidemic has been previously documented by our group.¹²

Unlike other countries,⁴⁰ we did not detect emerging *S. aureus* clones during the pandemic, as the prevalence of lineages remained consistent with that observed in the pre-pandemic era. However, we noticed a significant increase in strains carrying the *clfA* and *clfB* genes, a reduction of strains encoding *sdrE*, along with a rise in macrolide and methicillin antibiotic resistance genes (Table S5). This implies that these genes are increasing in prevalence across diverse lineages (Table S7), suggesting a genetic enrichment process rather than the emergence of dominant lineages during the pandemic period, as also evidenced by the phylogenetic analysis (Figure S2). This reflects an evolutionary scenario in which specific genes are convergently selected among diverse isolates, regardless of lineage, likely due to selective pressures during the COVID-19 infection.

The *clfA* and *clfB* genes are MSCRAMMs encoding the fibrinogen-binding clumping factors A and B, respectively. Fibrinogen is one of the most prevalent coagulation proteins in blood.¹⁴ ClfA is the major virulence factor responsible for *S. aureus* clumping in blood plasma,⁴¹ and ClfB interacts with cytokeratin 10 and loricrin facilitating *S. aureus* skin infection.⁴² Both ClfA and ClfB have been reported to be involved in bacterial and platelet aggregation.⁴¹ Interestingly, several reports documented an increase of fibrinogen production by SARS-CoV-2 virus.¹⁴ Therefore, our results suggest that the presence of *clfA* and *clfB* genes provided an advantage to *S. aureus* in the context of SARS-CoV-2 co-infection by enhancing fibrinogen binding. In consequence, *S. aureus* bloodstream isolates carrying the *clfA* and *clfB* genes were positively selected between 2020 and 2022. Despite using short-read sequencing, the pipeline employed unequivocally demonstrates a higher prevalence of *clfA* and *clfB* genes in the pandemic period. However, given the presence of duplicated regions within these genes, further analyses with long-read sequencing platforms could be appropriate.

Conversely, we found a reduced prevalence of the *sdrE* gene, which codes for an MSCRAMM that prevents *S. aureus* phagocytosis by sequestering the human complement factor H (CFH) on the surface of bacterial cells.³⁷ This is remarkable because it has been shown that the SARS-CoV-2 spike protein blocks CFH leading to a complement dysregulation on the human cell surface.⁴³ Therefore, the functional redundancy of *S. aureus* SdrE and the SARS-CoV-2 spike protein could explain the negative selection of *sdrE*. In the same line, it is important to note that *S. aureus* ClfA has also been found to have an anti-phagocytic effect.⁴⁴

Regarding *S. aureus* antibiotic resistance, some articles have emphasized the role of macrolides as adjunctive therapy for COVID-19 in certain patients,¹⁵ and the use of such antibiotics could allow selecting resistant strains. Macrolide resistance in staphylococci is mainly associated with mobile ARGs, which often correlates with methicillin resistance,⁴⁵ as also observed in our collection (Figure 2). These findings emphasize the evolving nature and impact of *S. aureus* infections in the COVID-19 pandemic era.

Limitations of the study

Our study elucidates evolutionary trends in *S. aureus* clinical isolates due to the selective pressure of the COVID-19 pandemic and reveals significant associations between lineages, antibiotic resistance genes, virulence factors, and clinical outcomes of bacteremia. However, the study could have benefited from a larger cohort of patients, including isolates from different countries and over a more extended period. This approach would allow to generalize our findings and to detect regional variations and long-term trends in *S. aureus* evolution. Furthermore, this research could have gained from utilizing long-read sequencing, which would enhance the detection of mobile genetic elements (plasmids and prophages) and improve the assembly of repeat-rich regions.

STAR★METHODS

Detailed methods are provided in the online version of this paper and include the following:

- KEY RESOURCES TABLE
- RESOURCE AVAILABILITY
 - Lead contact
 - Materials availability
 - Data and code availability
- EXPERIMENTAL MODEL AND STUDY PARTICIPANT DETAILS

- Patients and setting
- Clinical data
- Strain isolation and manipulation
- Ethics statement
- **METHOD DETAILS**
 - Whole-genome sequencing and *de novo* assembly
 - Isolate typing and *S. aureus* annotation
- **QUANTIFICATION AND STATISTICAL ANALYSIS**

SUPPLEMENTAL INFORMATION

Supplemental information can be found online at <https://doi.org/10.1016/j.isci.2024.110402>.

ACKNOWLEDGMENTS

This work was supported by the grant PI19/01911 from Instituto de Salud Carlos III (ISCIII). M.S.-O. and P.B. were the recipients of a Margarita Salas fellowship from the Ministerio de Universidades and a PFIS fellowship from the Instituto de Salud Carlos III, respectively. We are grateful to the staff of the Genomics Unit (CRG) for Illumina sequencing. We also want to acknowledge the CERCA Program/Generalitat de Catalunya.

AUTHOR CONTRIBUTIONS

Conceptualization, M.S.-O. and O.Q.P.; methodology, M.S.-O., I.E., O.G., and O.Q.P.; software, M.S.-O. and I.E.; investigation, M.S.-O., M.P., P.B., I.G.-S., M.A.-G., M.E., I.E., O.G., and O.Q.P.; data curation, M.S.-O. and M.P.; writing – original draft preparation, M.S.-O. and O.Q.P.; writing – review and editing, M.S.-O., M.P., P.B., I.G.-S., M.A.-G., M.E., I.E., O.G., and O.Q.P.; funding acquisition, O.Q.P. All authors have read and agreed to the published version of the manuscript.

DECLARATION OF INTERESTS

The authors declare no competing interests.

Received: January 25, 2024

Revised: May 10, 2024

Accepted: June 26, 2024

Published: June 28, 2024

REFERENCES

1. Viscoli, C. (2016). Bloodstream Infections: The peak of the iceberg. *Virulence* 7, 248–251. <https://doi.org/10.1080/21505594.2016.1152440>.
2. Gudiol, F., Aguado, J.M., Almirante, B., Bouza, E., Cercenado, E., Domínguez, M.Á., Gasch, O., Lora-Tamayo, J., Miró, J.M., Palomar, M., et al. (2015). Executive summary of the diagnosis and treatment of bacteremia and endocarditis due to *Staphylococcus aureus*. A clinical guideline from the Spanish Society of Clinical Microbiology and Infectious Diseases (SEIMC). *Enferm. Infecc. Microbiol. Clín.* 33, 626–632. <https://doi.org/10.1016/j.eimc.2015.03.014>.
3. Kern, W.V., and Rieg, S. (2020). Burden of bacterial bloodstream infection—a brief update on epidemiology and significance of multidrug-resistant pathogens. *Clin. Microbiol. Infect.* 26, 151–157. <https://doi.org/10.1016/j.cmi.2019.10.031>.
4. Wiggers, J.B., Xiong, W., and Daneman, N. (2016). Sending repeat cultures: is there a role in the management of bacteremic episodes? (SCRIBE study). *BMC Infect. Dis.* 16, 286. <https://doi.org/10.1186/s12879-016-1622-z>.
5. Khatib, R., Johnson, L.B., Fakhri, M.G., Riederer, K., Khosrovaneh, A., Shams Tabriz, M., Sharma, M., and Saeed, S. (2006). Persistence in *Staphylococcus aureus* bacteremia: incidence, characteristics of patients and outcome. *Scand. J. Infect. Dis.* 38, 7–14. <https://doi.org/10.1080/00365540500372846>.
6. Singer, M., Deutschman, C.S., Seymour, C.W., Shankar-Hari, M., Annane, D., Bauer, M., Bellomo, R., Bernard, G.R., Chiche, J.-D., Coopersmith, C.M., et al. (2016). The Third International Consensus Definitions for Sepsis and Septic Shock (Sepsis-3). *JAMA* 315, 801–810. <https://doi.org/10.1001/jama.2016.0287>.
7. van Hal, S.J., Jensen, S.O., Vaska, V.L., Espedido, B.A., Paterson, D.L., and Gosbell, I.B. (2012). Predictors of mortality in *Staphylococcus aureus* Bacteremia. *Clin. Microbiol. Rev.* 25, 362–386. <https://doi.org/10.1128/CMR.05022-11>.
8. Lee, A.S., de Lencastre, H., Garau, J., Kluytmans, J., Malhotra-Kumar, S., Peschel, A., and Harbarth, S. (2018). Methicillin-resistant *Staphylococcus aureus*. *Nat. Rev. Dis. Prim.* 4, 18033. <https://doi.org/10.1038/nrdp.2018.33>.
9. Recker, M., Laabei, M., Toleman, M.S., Reuter, S., Saunderson, R.B., Blane, B., Török, M.E., Ouadi, K., Stevens, E., Yokoyama, M., et al. (2017). Clonal differences in *Staphylococcus aureus* bacteraemia-associated mortality. *Nat. Microbiol.* 2, 1381–1388. <https://doi.org/10.1038/s41564-017-0001-x>.
10. Chertow, D.S., and Memoli, M.J. (2013). Bacterial coinfection in influenza: a grand rounds review. *JAMA* 309, 275–282. <https://doi.org/10.1001/jama.2012.194139>.
11. Falces-Romero, I., Bloise, I., García-Rodríguez, J., and Cendejas-Bueno, E.; SARS-CoV-2 Working Group (2023). *Staphylococcus aureus* bacteremia in patients with SARS-CoV-2 infection. *Med. Clin.* 160, 495–498. <https://doi.org/10.1016/j.medcle.2023.05.007>.
12. Gasch, O., Badia-Cebada, L., Carmezim, J., Vaqué, M., Pomar, V., Moreno, E., Marrón, A., Jiménez-Martínez, E., García-Quesada, M.J., García-Alarcón, X., et al. (2022). Effects of the COVID-19 Pandemic on Incidence and Epidemiology of Catheter-Related Bacteremia, Spain. *Emerg. Infect. Dis.* 28, 2181–2189. <https://doi.org/10.3201/eid2811.220547>.
13. Adalbert, J.R., Varshney, K., Tobin, R., and Pajaro, R. (2021). Clinical outcomes in patients co-infected with COVID-19 and *Staphylococcus aureus*: a scoping review. *BMC Infect. Dis.* 21, 985. <https://doi.org/10.1186/s12879-021-06616-4>.
14. Kangro, K., Wolberg, A.S., and Flick, M.J. (2022). Fibrinogen, Fibrin, and Fibrin Degradation Products in COVID-19. *Curr. Drug Targets* 23, 1593–1602. <https://doi.org/10.2174/138945012366220826162900>.

15. Sterenczak, K.A., Barrantes, I., Stahnke, T., Stachs, O., Fuellen, G., and Undre, N. (2020). Co-infections: testing macrolides for added benefit in patients with COVID-19. *Lancet Microbe* 1, e313. [https://doi.org/10.1016/S2666-5247\(20\)30170-1](https://doi.org/10.1016/S2666-5247(20)30170-1).
16. Souli, M., Ruffin, F., Choi, S.-H., Park, L.P., Gao, S., Lent, N.C., Sharma-Kuinkel, B.K., Thaden, J.T., Maskarinec, S.A., Wanda, L., et al. (2019). Changing Characteristics of *Staphylococcus aureus* Bacteremia: Results From a 21-Year, Prospective, Longitudinal Study. *Clin. Infect. Dis.* 69, 1868–1877. <https://doi.org/10.1093/cid/ciz112>.
17. Turnidge, J.D., Kotsanas, D., Munckhof, W., Roberts, S., Bennett, C.M., Nimmo, G.R., Coombs, G.W., Murray, R.J., Howden, B., Johnson, P.D.R., et al. (2009). *Staphylococcus aureus* bacteraemia: a major cause of mortality in Australia and New Zealand. *Med. J. Aust.* 191, 368–373. <https://doi.org/10.5694/j.1326-5377.2009.tb02841.x>.
18. Pérez-Montarelo, D., Viedma, E., Larrosa, N., Gómez-González, C., Ruiz de Gopegui, E., Muñoz-Gallego, I., San Juan, R., Fernández-Hidalgo, N., Almirante, B., and Chaves, F. (2018). Molecular Epidemiology of *Staphylococcus aureus* Bacteremia: Association of Molecular Factors With the Source of Infection. *Front. Microbiol.* 9, 2210. <https://doi.org/10.3389/fmicb.2018.02210>.
19. Park, K.-H., Greenwood-Quaintance, K.E., Uhl, J.R., Cunningham, S.A., Chia, N., Jeraldo, P.R., Sampathkumar, P., Nelson, H., and Patel, R. (2017). Molecular epidemiology of *Staphylococcus aureus* bacteremia in a single large Minnesota medical center in 2015 as assessed using MLST, core genome MLST and spa typing. *PLoS One* 12, e0179003. <https://doi.org/10.1371/journal.pone.0179003>.
20. Campbell, A.J., Mowlaboccus, S., Coombs, G.W., Daley, D.A., Al Yazidi, L.S., Phuong, L.K., Leung, C., Best, E.J., Webb, R.H., Voss, L., et al. (2022). Whole genome sequencing and molecular epidemiology of paediatric *Staphylococcus aureus* bacteraemia. *J. Glob. Antimicrob. Resist.* 29, 197–206. <https://doi.org/10.1016/j.jgar.2022.03.012>.
21. Mama, O.M., Aspiroz, C., Ruiz-Ripa, L., Ceballos, S., Iñiguez-Barrio, M., Cercenado, E., Azcona, J.M., López-Cerero, L., Seral, C., López-Calleja, A.I., et al. (2021). Prevalence and Genetic Characteristics of *Staphylococcus aureus* CC398 Isolates From Invasive Infections in Spanish Hospitals, Focusing on the Livestock-Independent CC398-MSSA Clade. *Front. Microbiol.* 12, 623108. <https://doi.org/10.3389/fmicb.2021.623108>.
22. Laumay, F., Benchetrit, H., Corvaglia, A.-R., van der Mee-Marquet, N., and François, P. (2021). The *Staphylococcus aureus* CC398 Lineage: An Evolution Driven by the Acquisition of Prophages and Other Mobile Genetic Elements. *Genes* 12, 1752. <https://doi.org/10.3390/genes12111752>.
23. Miller, C.E., Batra, R., Cooper, B.S., Patel, A.K., Klein, J., Otter, J.A., Kyraios, T., French, G.L., Tosas, O., and Edgeworth, J.D. (2012). An association between bacterial genotype combined with a high-vancomycin minimum inhibitory concentration and risk of endocarditis in methicillin-resistant *Staphylococcus aureus* bloodstream infection. *Clin. Infect. Dis.* 54, 591–600. <https://doi.org/10.1093/cid/cir858>.
24. Fernández-Hidalgo, N., Ribera, A., Larrosa, M.N., Viedma, E., Origián, J., de Alarcón, A., Fariñas, M.C., Sáez, C., Peña, C., Múñez, E., et al. (2018). Impact of *Staphylococcus aureus* phenotype and genotype on the clinical characteristics and outcome of infective endocarditis. A multicentre, longitudinal, prospective, observational study. *Clin. Microbiol. Infect.* 24, 985–991. <https://doi.org/10.1016/j.cmi.2017.12.002>.
25. Antonelli, A., Giani, T., Coppi, M., Di Pilato, V., Arena, F., Colavecchio, O.L., Conte, V., Santerre Henriksen, A., and Rossolini, G.M.; MRSA-HAP Study Group (2019). *Staphylococcus aureus* from hospital-acquired pneumonia from an Italian nationwide survey: activity of ceftobiprole and other anti-staphylococcal agents, and molecular epidemiology of methicillin-resistant isolates. *J. Antimicrob. Chemother.* 74, 3453–3461. <https://doi.org/10.1093/jac/dkz371>.
26. Munckhof, W.J., Nimmo, G.R., Carney, J., Schooneveldt, J.M., Huygens, F., Inman-Bamber, J., Tong, E., Morton, A., and Giffard, P. (2008). Methicillin-susceptible, non-multiresistant methicillin-resistant and multiresistant methicillin-resistant *Staphylococcus aureus* infections: a clinical, epidemiological and microbiological comparative study. *Eur. J. Clin. Microbiol. Infect. Dis.* 27, 355–364. <https://doi.org/10.1007/s10096-007-0449-3>.
27. Vázquez-Sánchez, D.A., Grillo, S., Carrera-Salinas, A., González-Díaz, A., Cuervo, G., Grau, I., Camoez, M., Martí, S., Berbel, D., Tubau, F., et al. (2022). Molecular Epidemiology, Antimicrobial Susceptibility, and Clinical Features of Methicillin-Resistant *Staphylococcus aureus* Bloodstream Infections over 30 Years in Barcelona, Spain (1990–2019). *Microorganisms* 10, 2401. <https://doi.org/10.3390/microorganisms10122401>.
28. Dupper, A.C., Sullivan, M.J., Chacko, K.I., Mishkin, A., Ciferri, B., Kumaresh, A., Berbel Caban, A., Oussenko, I., Beckford, C., Zeitouni, N.E., et al. (2019). Blurred Molecular Epidemiological Lines Between the Two Dominant Methicillin-Resistant *Staphylococcus aureus* Clones. *Open Forum Infect. Dis.* 6, ofz302. <https://doi.org/10.1093/ofid/ofz302>.
29. Smith, J.T., Eckhardt, E.M., Hansel, N.B., Eliato, T.R., Martin, I.W., and Andam, C.P. (2021). Genomic epidemiology of methicillin-resistant and -susceptible *Staphylococcus aureus* from bloodstream infections. *BMC Infect. Dis.* 21, 589. <https://doi.org/10.1186/s12879-021-06293-3>.
30. Chen, C., and Hooper, D.C. (2018). Effect of *Staphylococcus aureus* Tet38 native efflux pump on in vivo response to tetracycline in a murine subcutaneous abscess model. *J. Antimicrob. Chemother.* 73, 720–723. <https://doi.org/10.1093/jac/dkx432>.
31. Monecke, S., Coombs, G., Shore, A.C., Coleman, D.C., Akpaka, P., Borg, M., Chow, H., Ip, M., Jatzwauk, L., Jonas, D., et al. (2011). A field guide to pandemic, epidemic and sporadic clones of methicillin-resistant *Staphylococcus aureus*. *PLoS One* 6, e17936. <https://doi.org/10.1371/journal.pone.0017936>.
32. Rasmussen, G., Monecke, S., Ehrlich, R., and Söderquist, B. (2013). Prevalence of clonal complexes and virulence genes among commensal and invasive *Staphylococcus aureus* isolates in Sweden. *PLoS One* 8, e77477. <https://doi.org/10.1371/journal.pone.0077477>.
33. Sieber, R.N., Urth, T.R., Petersen, A., Møller, C.H., Price, L.B., Skov, R.L., Larsen, A.R., Stegger, M., and Larsen, J. (2020). Phage-Mediated Immune Evasion and Transmission of Livestock-Associated Methicillin-Resistant *Staphylococcus aureus* in Humans. *Emerg. Infect. Dis.* 26, 2578–2585. <https://doi.org/10.3201/eid2611.201442>.
34. Cheung, G.Y.C., Bae, J.S., and Otto, M. (2021). Pathogenicity and virulence of *Staphylococcus aureus*. *Virulence* 12, 547–569. <https://doi.org/10.1080/21505594.2021.1878688>.
35. Pinchuk, I.V., Beswick, E.J., and Reyes, V.E. (2010). Staphylococcal Enterotoxins. *Toxins* 2, 2177–2197. <https://doi.org/10.3390/toxins2082177>.
36. Betley, M.J., and Mekalanos, J.J. (1985). Staphylococcal enterotoxin A is encoded by phage. *Science* 229, 185–187. <https://doi.org/10.1126/science.3160112>.
37. Wójcik-Bojek, U., Różalska, B., and Sadowska, B. (2022). *Staphylococcus aureus*-A Known Opponent against Host Defense Mechanisms and Vaccine Development-Do We Still Have a Chance to Win? *Int. J. Mol. Sci.* 23, 948. <https://doi.org/10.3390/ijms23020948>.
38. Fey, P.D., Saïd-Salim, B., Rupp, M.E., Hinrichs, S.H., Boxrud, D.J., Davis, C.C., Kreiswirth, B.N., and Schlievert, P.M. (2003). Comparative molecular analysis of community- or hospital-acquired methicillin-resistant *Staphylococcus aureus*. *Antimicrob. Agents Chemother.* 47, 196–203. <https://doi.org/10.1128/AAC.47.1.196-203.2003>.
39. Shohayeb, M., El-Banna, T., Elsayw, L.E., and El-Bouseary, M.M. (2023). Panton-Valentine Leukocidin (PVL) genes may not be a reliable marker for community-acquired MRSA in the Dakahlia Governorate, Egypt. *BMC Microbiol.* 23, 315. <https://doi.org/10.1186/s12866-023-03065-8>.
40. Gu, J., Shen, S., Xiong, M., Zhao, J., Tian, H., Xiao, X., and Li, Y. (2023). ST7 Becomes One of the Most Common *Staphylococcus aureus* Clones After the COVID-19 Epidemic in the City of Wuhan, China. *Infect. Drug Resist.* 16, 843–852. <https://doi.org/10.2147/IDR.S401069>.
41. O'Brien, L., Kerrigan, S.W., Kaw, G., Hogan, M., Penades, J., Litt, D., Fitzgerald, D.J., Foster, T.J., and Cox, D. (2002). Multiple mechanisms for the activation of human platelet aggregation by *Staphylococcus aureus*: roles for the clumping factors ClfA and ClfB, the serine-aspartate repeat protein SdrE and protein A. *Mol. Microbiol.* 44, 1033–1044. <https://doi.org/10.1046/j.1365-2958.2002.02935.x>.
42. Lacey, K.A., Mulcahy, M.E., Towell, A.M., Geoghegan, J.A., and McLoughlin, R.M. (2019). Clumping factor B is an important virulence factor during *Staphylococcus aureus* skin infection and a promising vaccine target. *PLoS Pathog.* 15, e1007713. <https://doi.org/10.1371/journal.ppat.1007713>.
43. Yu, J., Gerber, G.F., Chen, H., Yuan, X., Chaturvedi, S., Braunstein, E.M., and Brodsky, R.A. (2022). Complement dysregulation is associated with severe COVID-19 illness. *Haematologica* 107, 1095–1105. <https://doi.org/10.3324/haematol.2021.279155>.
44. Hair, P.S., Echague, C.G., Sholl, A.M., Watkins, J.A., Geoghegan, J.A., Foster, T.J., and Cunnion, K.M. (2010). Clumping Factor A Interaction with Complement Factor I Increases C3b Cleavage on the Bacterial Surface of *Staphylococcus aureus* and Decreases Complement-Mediated

- Phagocytosis. *Infect. Immun.* 78, 1717–1727. <https://doi.org/10.1128/IAI.01065-09>.
45. Serra, N., Di Carlo, P., Andriolo, M., Mazzola, G., Diprima, E., Rea, T., Anastasia, A., Fasciana, T.M.A., Pipitò, L., Capra, G., et al. (2023). *Staphylococcus aureus* and Coagulase-Negative Staphylococci from Bloodstream Infections: Frequency of Occurrence and Antimicrobial Resistance, 2018–2021. *Life* 13, 1356. <https://doi.org/10.3390/1ife13061356>.
46. Seemann, T. (2014). Prokka: rapid prokaryotic genome annotation. *Bioinformatics* 30, 2068–2069. <https://doi.org/10.1093/bioinformatics/btu153>.
47. Chklovskii, A., Parks, D.H., Woodcroft, B.J., and Tyson, G.W. (2023). CheckM2: a rapid, scalable and accurate tool for assessing microbial genome quality using machine learning. *Nat. Methods* 20, 1203–1212. <https://doi.org/10.1038/s41592-023-01940-w>.
48. Larsen, M.V., Cosentino, S., Rasmussen, S., Friis, C., Hasman, H., Marvig, R.L., Jelsbak, L., Sicheritz-Pontén, T., Ussery, D.W., Aarestrup, F.M., and Lund, O. (2012). Multilocus sequence typing of total-genome-sequenced bacteria. *J. Clin. Microbiol.* 50, 1355–1361. <https://doi.org/10.1128/JCM.06094-11>.
49. Raghuram, V., Alexander, A.M., Loo, H.Q., Petit, R.A., Goldberg, J.B., and Read, T.D. (2022). Species-Wide Phylogenomics of the *Staphylococcus aureus* Agr Operon Revealed Convergent Evolution of Frameshift Mutations. *Microbiol. Spectr.* 10, e0133421. <https://doi.org/10.1128/spectrum.01334-21>.
50. Kaya, H., Hasman, H., Larsen, J., Stegger, M., Johannesen, T.B., Allesøe, R.L., Lemvig, C.K., Aarestrup, F.M., Lund, O., and Larsen, A.R. (2018). SCCmecFinder, a Web-Based Tool for Typing of Staphylococcal Cassette Chromosome *mec* in *Staphylococcus aureus* Using Whole-Genome Sequence Data. *mSphere* 3, e00612-17. <https://doi.org/10.1128/mSphere.00612-17>.
51. Bortolaia, V., Kaas, R.S., Ruppe, E., Roberts, M.C., Schwarz, S., Cattoir, V., Philippon, A., Allesøe, R.L., Rebelo, A.R., Florensa, A.F., et al. (2020). ResFinder 4.0 for predictions of phenotypes from genotypes. *J. Antimicrob. Chemother.* 75, 3491–3500. <https://doi.org/10.1093/jac/dkaa345>.
52. Robertson, J., and Nash, J.H.E. (2018). MOB-suite: software tools for clustering, reconstruction and typing of plasmids from draft assemblies. *Microb. Genom.* 4, e000206. <https://doi.org/10.1099/mgen.0.000206>.
53. Carattoli, A., Zankari, E., García-Fernández, A., Voldby Larsen, M., Lund, O., Villa, L., Møller Aarestrup, F., and Hasman, H. (2014). In silico detection and typing of plasmids using PlasmidFinder and plasmid multilocus sequence typing. *Antimicrob. Agents Chemother.* 58, 3895–3903. <https://doi.org/10.1128/AAC.02412-14>.
54. Page, A.J., Cummins, C.A., Hunt, M., Wong, V.K., Reuter, S., Holden, M.T.G., Fookes, M., Falush, D., Keane, J.A., and Parkhill, J. (2015). Roary: rapid large-scale prokaryote pan genome analysis. *Bioinformatics* 31, 3691–3693. <https://doi.org/10.1093/bioinformatics/btv421>.
55. Akhter, S., Aziz, R.K., and Edwards, R.A. (2012). PhiSpy: a novel algorithm for finding prophages in bacterial genomes that combines similarity- and composition-based strategies. *Nucleic Acids Res.* 40, e126. <https://doi.org/10.1093/nar/gks406>.
56. Edgar, R.C. (2010). Search and clustering orders of magnitude faster than BLAST. *Bioinformatics* 26, 2460–2461. <https://doi.org/10.1093/bioinformatics/btq461>.
57. Altschul, S.F., Gish, W., Miller, W., Myers, E.W., and Lipman, D.J. (1990). Basic local alignment search tool. *J. Mol. Biol.* 215, 403–410. [https://doi.org/10.1016/S0022-2836\(05\)80360-2](https://doi.org/10.1016/S0022-2836(05)80360-2).
58. Thompson, J.D., Higgins, D.G., and Gibson, T.J. (1994). CLUSTAL W: improving the sensitivity of progressive multiple sequence alignment through sequence weighting, position-specific gap penalties and weight matrix choice. *Nucleic Acids Res.* 22, 4673–4680. <https://doi.org/10.1093/nar/22.22.4673>.
59. Letunic, I., and Bork, P. (2019). Interactive Tree Of Life (iTOL) v4: recent updates and new developments. *Nucleic Acids Res.* 47, W256–W259. <https://doi.org/10.1093/nar/gkz2239>.
60. Charlson, M.E., Pompei, P., Ales, K.L., and MacKenzie, C.R. (1987). A new method of classifying prognostic comorbidity in longitudinal studies: development and validation. *J. Chron. Dis.* 40, 373–383. [https://doi.org/10.1016/0021-9681\(87\)90171-8](https://doi.org/10.1016/0021-9681(87)90171-8).
61. Friedman, N.D., Kaye, K.S., Stout, J.E., McGarry, S.A., Trivette, S.L., Briggs, J.P., Lamm, W., Clark, C., MacFarquhar, J., Walton, A.L., et al. (2002). Health care-associated bloodstream infections in adults: a reason to change the accepted definition of community-acquired infections. *Ann. Intern. Med.* 137, 791–797. <https://doi.org/10.7326/0003-4819-137-10-200211190-00007>.
62. Sweet, T., Sindi, S., and Sstrom, M. (2023). Going through phages: a computational approach to revealing the role of prophage in *Staphylococcus aureus*. *Access Microbiol.* 5, acmi000424. <https://doi.org/10.1099/acmi.0.000424>.
63. Goerke, C., Pantucek, R., Holtfreter, S., Schulte, B., Zink, M., Grumann, D., Bröker, B.M., Doskar, J., and Wolz, C. (2009). Diversity of prophages in dominant *Staphylococcus aureus* clonal lineages. *J. Bacteriol.* 191, 3462–3468. <https://doi.org/10.1128/JB.01804-08>.

STAR★METHODS

KEY RESOURCES TABLE

REAGENT or RESOURCE	SOURCE	IDENTIFIER
Bacterial and virus strains		
<i>S. aureus</i> strains (n = 339)	This paper	see Data S1
Chemicals, peptides, and recombinant proteins		
Columbia Agar with 5% Sheep Blood plates	Biomérieux	Cat#411617
Lysostaphin	Merck	Cat#L7386
Critical commercial assays		
DNeasy Blood & Tissue Purification Kit	Qiagen	Cat#69504
Nextera XT DNA Sample Preparation Kit	Illumina	Cat#FC-131-1024
Deposited data		
Illumina raw reads	This paper	PRJNA1055690
Software and algorithms		
FastQC	https://github.com/s-andrews/FastQC	N/A
TrimGalore	https://github.com/FelixKrueger/TrimGalore	N/A
Shovill	https://github.com/tseemann/shovill	N/A
Prokka	https://github.com/tseemann/prokka	Seemann ⁴⁶
CheckM2	https://github.com/chklovski/CheckM2	Chklovski et al. ⁴⁷
MLST	https://bitbucket.org/genomicepidemiology/mlst.git/src	Larsen et al. ⁴⁸
SpaTyper	https://github.com/HCGB-IGTP/spaTyper	N/A
AgrVATE	https://github.com/VishnuRaghuram94/AgrVATE	Raghuram et al. ⁴⁹
SCCmecFinder	https://cge.food.dtu.dk/services/SCCmecFinder/	Kaya et al. ⁵⁰
Abricate	https://github.com/tseemanN/Abricate	N/A
ResFinder	https://bitbucket.org/genomicepidemiology/resfinder/src/master/	Bortolaia et al. ⁵¹
MOB-suite	https://github.com/phac-nml/mob-suite	Robertson and Nash, ⁵²
PlasmidFinder	https://bitbucket.org/genomicepidemiology/plasmidfinder/src/master/	Carattoli et al. ⁵³
Roary	https://github.com/sanger-pathogens/Roary	Page et al. ⁵⁴
PhiSpy	https://github.com/linsalrob/PhiSpy	Akhter et al. ⁵⁵
Usearch	https://www.drive5.com/usearch/	Edgar ⁵⁶
BLASTP	https://blast.ncbi.nlm.nih.gov/Blast.cgi	Altschul et al. ⁵⁷
Snippy	https://github.com/tseemann/snippy	N/A
CLUSTALW	https://www.ebi.ac.uk/jdispatcher/msa/clustalo	Thompson et al. ⁵⁸
iTOL	https://itol.embl.de/	Letunic and Bork ⁵⁹

RESOURCE AVAILABILITY

Lead contact

Further information and requests for resources should be directed to and will be fulfilled by the lead contact, Oscar Q. Pich (ouqijada@tauli.cat).

Materials availability

Materials obtained in this study are available from the [lead contact](#) upon reasonable request.

Data and code availability

- All data is available in this paper as [supplemental information](#). Sequence data generated in this study have been deposited in the NCBI database with the following access number: PRJNA1055690.

- This paper does not report original code.
- Any additional information related to this paper is available from the [lead contact](#) upon request.

EXPERIMENTAL MODEL AND STUDY PARTICIPANT DETAILS

Patients and setting

All consecutive adult patients (≥ 18 years) diagnosed with *S. aureus* bloodstream infection from July 2014 to December 2022 at the Parc Taulí University Hospital (Sabadell, Spain) were retrospectively included in this study. Patients' sex is included in [Data S1](#). Race of patients was not recorded in this study.

Clinical data

Clinical information was recorded including patient demographics, comorbidities and other clinical characteristics, source of bacteremia, place of acquisition, severity of sepsis, antibiotic therapy and infection outcomes. The modified Charlson score⁶⁰ was used to assess patient morbidities. Setting of acquisition was classified according to modified Friedman criteria⁶¹ as: community, in-hospital acquired or healthcare-related. 30-day mortality was considered as any death within the first month after the bloodstream infection onset. Persistent bacteremia was defined as the presence of positive blood cultures after 72 h of appropriate antibiotic therapy. Septic embolism was determined as the presence of one or more diagnosed secondary foci as a result of bacterial spread through blood. Strains isolated from March 14th 2020 (Spain's lockdown start) onwards were considered as pandemic clones. These data are available in [Data S1](#).

Strain isolation and manipulation

For each patient, only the first episode of *S. aureus* bacteremia was included in the analysis. Blood cultures were processed using the BACT/ALERT automated system (bioMérieux) following standardized procedures. *S. aureus* strains were identified by using mass spectrometry technology (MALDI-TOF MS, Bruker). *S. aureus* single colonies were frozen and stored at -80°C . Antibiotic susceptibility testing was assessed by microdilution methodology according to standardized protocols using the MicroScan WalkAway system (Beckman Coulter).

Ethics statement

The Ethics Committee for Investigation with medicinal products (CEIm) of the Parc Taulí University Hospital approved the implementation of this study (2023/5088, approved on 6 October 2023). The requirement for informed written consent was waived given the retrospective nature of the study. Patient identification was encoded, complying with the requirements of the Spanish Organic Law on Data Protection 15/1999.

METHOD DETAILS

Whole-genome sequencing and *de novo* assembly

DNA extraction

S. aureus isolates were grown on Columbia Agar with 5% Sheep Blood plates (bioMérieux) at 37°C . Total DNA was purified using the DNeasy Blood & Tissue Purification Kit (Qiagen) following the manufacturer's instructions. Cell lysis was achieved by pre-incubating bacterial colonies in Phosphate-buffered saline (PBS) containing $100\ \mu\text{g}/\text{mL}$ lysostaphin (Merck) at 37°C for 30 min. DNA quality was assessed using a NanoDrop device (Thermo Fisher Scientific) and a Qubit 2.0 fluorometer (Thermo Fisher Scientific).

DNA sequencing

Libraries for sequencing were prepared with the Nextera XT DNA Sample Preparation Kit (Illumina). Whole-genome sequencing was performed using paired-end sequencing on an Illumina HiSeq 2500 and NovaSeq 600 sequencers available at the Genomics Unit of the Center de Regulació Genòmica (CRG, Barcelona). Whole-genome sequencing data are available at National Center for Biotechnology Information (NCBI) under the accession number PRJNA1055690.

Quality control

The quality of the raw sequencing reads was checked with FastQC (<https://www.bioinformatics.babraham.ac.uk/projects/fastqc/>, accessed on December 2023). Read pre-processing and filtering were performed with TrimGalore (https://www.bioinformatics.babraham.ac.uk/projects/trim_galore/, accessed on December 2023) by shaving the sequencing adapters, trimming the initial 20 bp poor-quality positions and using a Phred score ≥ 20 limit.

De novo assembly

The trimmed paired-end reads were assembled *de novo* using shovill (<https://github.com/tseemann/shovill>, accessed on December 2023), and annotated with prokka⁴⁶ against the COG, HAMAP and Pfam databases and using the *S. aureus* NCTC 8325 [GenBank: NC_007795] proteome as the reference. CheckM2 was finally used for assessing the quality of assemblies.⁴⁷

Isolate typing and *S. aureus* annotation

Isolate typing

Multilocus sequence typing (MLST) was carried out on the assembled scaffolds using the MLST software.⁴⁸ Sequence Types (ST) and Clonal Complexes (CC) were deduced from the *S. aureus* PubMLST database grouping the *arcC*, *aroE*, *glpF*, *gmk*, *pta*, *tpi* and *yqiL* gene types. spaTyper was used to assign *spa* types according to the Ridom Spa Server database guidelines (<https://github.com/HCGB-IGTP/spaTyper>, accessed on December 2023), AgrVATE was used for *agr* typing⁴⁹ and SCCmec-types were obtained using SCCmecFinder.⁵⁰

Antibiotic resistance genes and virulence factors

Putative ARG and VF were predicted on the assembled scaffolds with ABRicate (<https://github.com/tseemann/abricate>, accessed on December 2023) using the in-built NCBI AMRFinderPlus database and Virulence Factor Database (VFDB) and otherwise default parameters, respectively. Prediction of mutations conferring antimicrobial resistance was conducted using ResFinder against *Staphylococcus aureus* database.⁵¹ Strains were considered as Panton-Valentine leukocidin (PVL) positive when both *lukF* and *lukS* genes were predicted on the same genome.

Plasmid prediction

Plasmid scaffolds were identified using MOB-recon and mobility was predicted based on the MOB-typer module.⁵² PlasmidFinder software from Center for Genomic Epidemiology (CGE) was used for *rep* typing⁵³ and roary for identifying plasmid core genes.⁵⁴

Prophage prediction

Prophage prediction was performed as described recently for other *S. aureus* genomes.⁶² Prophage regions were detected in assembled scaffolds using PhiSpy⁵⁵ and Prophage clustering was carried out with usearch⁵⁶ so that sequences showing 90% similarity along their 90% length were counted as the same. Integrase detection and typing was assessed with BLASTP⁵⁷ using previously reported integrase sequences⁶³ as queries and limiting the e-value to $1e^{-20}$ and query coverage to >75%. Each putative integrase identified in the prophage regions was classified into an integrase group according to the query with the lowest e-value in the BLASTP analysis.

Phylogenetic inference

Phylogenetic analysis was performed using core genome alignments based on single nucleotide polymorphisms (SNPs) called by snippy (<https://github.com/tseemann/snippy>, accessed on April 2024) against the *S. aureus* NCTC 8325 genome [GenBank: NC_007795]. A Neighbor Joining (NJ) tree was constructed using CLUSTALW with 100 bootstrap replicates⁵⁸ and visualized with the iTOL online tool.⁵⁹

QUANTIFICATION AND STATISTICAL ANALYSIS

Mann-Whitney U (MWU) test was used for continuous variables and Fisher's exact test (FT) for categorical variables. For clonal associations, MWU was first applied to determine biased distributions of lineages when analyzing a specific genetic feature. If the lineage distributions differed significantly when compared to global frequencies, FT was independently applied to determine the association of each feature with specific lineages. Clonal associations were only computed for strains with known lineage. Always a *p*-value threshold of 0.05 was considered as significant. Statistical analyses were performed using custom Python scripts.